ISSN 1674-1056
http://cpb.iphy.ac.cn
http://iopscience.iop.org/cpb
中国物理 B
Chinese Physics
中国物理
Chinese Physics B

Valley-polarized pumping current in zigzag graphene nanoribbons with different spatial symmetries

Zhizhou Yu(俞之舟), Fuming Xu(许富明)

Citation: Chin. Phys. B . 2018, 27(12): 127203. **doi:** 10.1088/1674-1056/27/12/127203
Journal homepage: http://cpb.iphy.ac.cn; http://iopscience.iop.org/cpb

What follows is a list of articles you may be interested in

The magneto-thermoelectric effect of graphene with intra-valley scattering

Wenye Duan(段文晔), Junfeng Liu(刘军丰), Chao Zhang(张潮), Zhongshui Ma(马中水)
Chin. Phys. B . 2018, 27(9): 097204. **doi:** 10.1088/1674-1056/27/9/097204

Transport properties in monolayer-bilayer-monolayer graphene planar junctions

Kai-Long Chu(储开龙), Zi-Bo Wang(王孜博), Jiao-Jiao Zhou(周娇娇), Hua Jiang(江华)
Chin. Phys. B . 2017, 26(6): 067202. **doi:** 10.1088/1674-1056/26/6/067202

High temperature characteristics of bilayer epitaxial graphene field-effect transistors on SiC Substrate

Ze-Zhao He(何泽召), Ke-Wu Yang(杨克武), Cui Yu(蔚翠), Qing-Bin Liu(刘庆彬), Jing-Jing Wang(王晶晶), Jia Li(李佳), Wei-Li Lu(芦伟立), Zhi-Hong Feng(冯志红), Shu-Jun Cai(蔡树军)
Chin. Phys. B . 2016, 25(6): 067206. **doi:** 10.1088/1674-1056/25/6/067206

A self-powered sensitive ultraviolet photodetector based on epitaxial graphene on silicon carbide

Jiao Huang(黄郊), Li-Wei Guo(郭丽伟), Wei Lu(芦伟), Yong-Hui Zhang(张永晖), Zhe Shi(史哲), Yu-Ping Jia(贾玉萍), Zhi-Lin Li(李治林), Jun-Wei Yang(杨军伟), Hong-Xiang Chen(陈洪祥), Zeng-Xia Mei(梅增霞), Xiao-Long Chen(陈小龙)
Chin. Phys. B . 2016, 25(6): 067205. **doi:** 10.1088/1674-1056/25/6/067205

Adiabatic quantum pump in a zigzag graphene nanoribbon junction

Zhang Lin
Chin. Phys. B . 2015, 24(11): 117202. **doi:** 10.1088/1674-1056/24/11/117202

SPECIAL TOPIC — 60th Anniversary of the Department of Physics at the Nanjing Normal University

Valley-polarized pumping current in zigzag graphene nanoribbons with different spatial symmetries*

Zhizhou Yu(俞之舟)[1,†] and Fuming Xu(许富明)[2]

[1] Center for Quantum Transport and Thermal Energy Science, School of Physics and Technology, Nanjing Normal University, Nanjing 210023, China
[2] College of Physics and Energy, Shenzhen University, Shenzhen 518060, China

(Received 27 August 2018; revised manuscript received 5 October 2018; published online 10 November 2018)

We numerically investigate the valley-polarized current in symmetric and asymmetric zigzag graphene nanoribbons (ZGNRs) by the adiabatic pump, and the effect of spatial symmetry is considered by introducing different pumping regions. It is found that pumping potentials with the symmetry $V_p(x,y) = V_p(-x,y)$ can generate the largest valley-polarized current. The valley-polarized currents I^L_{13} with the pumping potential symmetry $V_p(x,y) = V_p(x,-y)$ and I^L_{14} with $V_p(x,y) = V_p(-x,-y)$ of symmetric ZGNRs are much smaller than those of asymmetric ZGNRs. We also find I^L_{13} and I^L_{14} of symmetric ZGNRs decrease and increase with the increasing pumping amplitude, respectively. Moreover, the dephasing effect from the electron–phonon coupling within the Buttiker dephasing scheme is introduced. The valley-polarized current of the symmetric ZGNRs with $V_p(x,y) = V_p(x,-y)$ increases with the increase of the dephasing strength while that with $V_p(x,y) = V_p(-x,-y)$ decreases as the dephasing strength increases.

Keywords: valley polarization, charge pump, graphene, quantum transport

PACS: 72.80.Vp, 73.63.–b, 73.23.–b, 85.75.–d **DOI:** 10.1088/1674-1056/27/12/127203

1. Introduction

Valleytronics has attracted much attention in the field of condensed matter physics, which aims to manipulate and control the valley degree of freedom of electrons in addition to charge and spin in order to carry and process information.[1–14] In general, a local minimum (maximum) of the conduction (valence) band is referred to as the valley. Recently, valleytronics has been widely enabled with the rapid development in fabricating the hexagonal two-dimensional (2D) materials, such as graphene and monolayer transition metal dichalcogenides (TMDCs) whose electronic properties can be characterized by two inequivalent valleys at the band edge, namely, the K and K' points in the first Brillouin zone.[1,2,6,12] In particular, a valley filter was first proposed in a ballistic point contact with one-dimensional (1D) zigzag graphene nanoribbons (ZGNRs) and the valley polarity can be inverted by a gate voltage on the point contact region.[1] The valley Hall effect that electrons in different valleys flow to opposite directions driven by an in-plain electric field was reported in graphene superlattices with broken inversion symmetry.[2,6]

One of the fundamental goals in valleytronics is the generation of pure valley current and valley-polarized current in 2D materials. Tarucha and coworkers detected the pure valley current in bilayer graphene by inducing the Berry curvature using a perpendicular electric field to break the spatial inversion symmetry.[15] The photoinduced valley-polarized current has been theoretically proposed in the monolayer TMDC by external electric field.[16,17] Moreover, the quantum parametric pump is an efficient way to generate dc currents through nanostructure by periodically varying two or more system parameters.[18–22] It has been widely used in many 2D materials.[23–27] A quantized charge pump based on massive Dirac electrons has been realized in graphene theoretically which is originated from the topologically protected edge states.[28] Recently, the pure bulk valley current was generated through pumping in a graphene mechanical resonator with cyclic deformations in the suspended region.[29] A pure valley current was also proposed by quantum pumping in a strain-engineered graphene in the presence of electric potential barriers and ferromagnetic fields.[30]

In this paper, the valley-polarized current in ZGNRs based devices generated by the adiabatic pump is studied. In order to study the effect of spatial symmetry of the pumping potential on the valley-polarized current, different pumping regions are considered. It is found that the pumped current induced by the pumping potentials with the symmetry $V_p(x,y) = V_p(-x,y)$ exhibits the largest value. We also find the pumping current with $V_p(x,y) = V_p(x,-y)$ decreases with the increase of pumping amplitude while that with $V_p(x,y) = V_p(-x,-y)$ increases with the increasing pumping amplitude. Moreover, the dephasing effect from the electron–phonon coupling is studied for the valley-polarized pumping current by using the Büttiker

*Project supported by the National Natural Science Foundation of China (Grant Nos. 11704190, 11874221, and 11504240) and the Natural Science Foundation of Jiangsu Province, China (Grant No. BK20171030).

†Corresponding author. E-mail: yuzhizhou@njnu.edu.cn

© 2018 Chinese Physical Society and IOP Publishing Ltd

dephasing scheme.

2. Model and formalism

Previous theoretical studies on 1D graphene nanoribbons have shown that for armchair nanoribbons, each propagating mode is constructed by the mixed states of both valleys, while the lowest propagating mode of ZGNRs is only contributed by a single valley, which means that the valley index is not well defined for the armchair graphene nanoribbons.[1] Therefore, ZGNRs are chosen to study the valley polarization of current in our present work. In the tight-binding approximation, the Hamiltonian of ZGNRs can be written as (here we set $\hbar = e = 1$ for simplicity),

$$H = -t_0 \sum_{\langle i,j \rangle} c_i^{\dagger} c_j + \text{H.c.} + \sum_{m \in k} V_k(t) c_m c_m^{\dagger}, \tag{1}$$

where c_i ($c_i^{\dagger}$) annihilates (creates) an electron on site i of ZGNRs. $\langle \cdots \rangle$ refers to the nearest-neighboring sites and t_0 is the nearest neighbor hopping energy which is set to be 2.7 eV.[31] $V_k(t) = V_0 + V_{\text{p}} \cos(\omega t + \phi_k)$ with V_0 and V_{p} the amplitudes of the static and pumping potential, respectively. Here, ω is the pumping frequency and ϕ_k is the initial phase of the time-varying potential. Two pumping potentials with different initial phases should be introduced in order to generate the pumping current and the potentials are applied in different regions k ($k = 1, 2, 3, 4$) as shown in Fig. 1(a).

For the adiabatic electron pump, the average current flowing through lead α due to the slow variation of system parameter V_k in one period is given by[15]

$$I_{\alpha}^{\text{p}} = \frac{1}{\tau} \int_0^{\tau} \mathrm{d}t \frac{\mathrm{d}Q_{\alpha}}{\mathrm{d}t}, \tag{2}$$

where $\tau = 2\pi/\omega$ is the variation period of potential V_k and $\mathrm{d}Q_{\alpha}$ is the pumped charge passing through lead α due to the change of system parameters which can be given by[17,32]

$$\frac{\mathrm{d}Q_{\alpha}}{\mathrm{d}t} = \int \frac{\mathrm{d}E}{2\pi} (-\partial_E f) \text{Tr} \left[\Gamma_{\alpha} G^{\text{r}} \frac{\mathrm{d}V_t}{\mathrm{d}t} G^{\text{a}} \right]. \tag{3}$$

Here, f is the Fermi–Dirac distribution and $V_t = \sum_k V_k(t)$. The instantaneous retarded Green's function G^{r} in real space is defined as

$$G^{\text{r}} = [E - H(t) - \Sigma^{\text{r}}]^{-1}, \tag{4}$$

with Σ^{r} the self-energy due to the leads. $\Gamma_{\alpha} = \text{i}[\Sigma_{\alpha}^{\text{r}} - \Sigma_{\alpha}^{\text{a}}]$ is the line-width function of lead α.

By using the variable substitution, the integration of Eq. (2) can be presented as,

$$I_{\alpha}^{\text{p}} = \frac{1}{2\pi} \int_0^{2\pi/\omega} i_{\alpha}(\omega t) \mathrm{d}(\omega t) = \frac{1}{2\pi} \int_0^{2\pi} i_{\alpha}(u) \mathrm{d}(u). \tag{5}$$

Therefore, the integration does not involve the frequency ω and we can choose $\omega = 1$ in our calculation for simplicity.

By combining Eqs. (2) and (3), the pumping current can be written as[17]

$$I_{\alpha}^{\text{p}} = \int_0^{2\pi} \mathrm{d}t \int \frac{\mathrm{d}E}{2\pi} (-\partial_E f) \text{Tr} \left[\Gamma_{\alpha} G^{\text{r}} \frac{\mathrm{d}V_t}{\mathrm{d}t} G^{\text{a}} \right]. \tag{6}$$

From the band structure of ZGNRs as plotted in Fig. 1(b), it has been reported that the momentum and valley index of electrons in the first subband are locked together which is independent of the ribbon width. As a result, the left-moving electrons in ZGNRs has valley index K while the right-moving electrons have valley index K'. Therefore, the pumping current with the pumping potential in the first subband of ZGNRs is fully valley polarized. The positive pumping current in the left (right) lead is a valley current with K (K') index while a negative pumping current in the left (right) lead is contributed by the valley index K' (K).

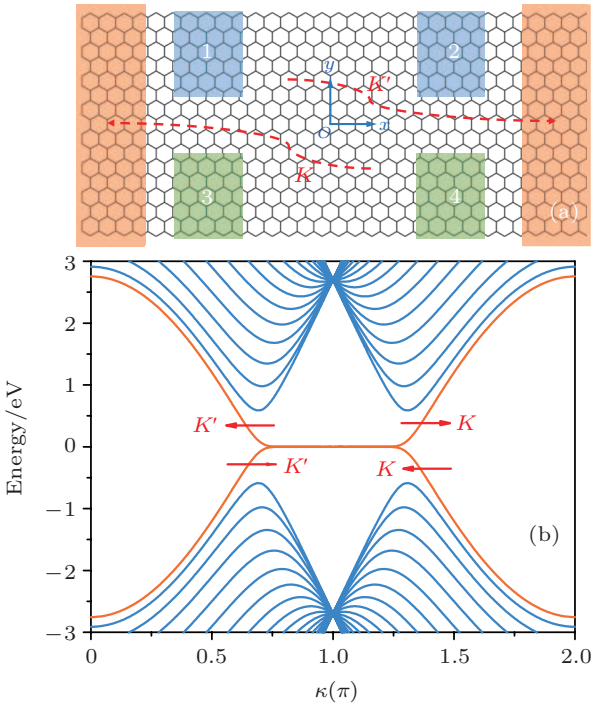


Fig. 1. (color online) (a) Schematic diagram of ZGNRs with two semi-infinite leads (orange shadow). Four pumping regions are represented by blue and green shadows in the central region. The origin of the axis is set to be the center of ZGNRs. (b) Band structure of ZGNRs with a width of 4.1 nm. The first subbands are highlighted with orange color and the arrows for different valley indices K and K' denote the moving directions of electrons.

In order to study the dephasing effect from the electron–phonon coupling, fictitious voltage probes are introduced into the graphene nanoribbons to model the influence of phase relaxing scattering proposed by Büttiker, which can be described by an on-site self-energy term Σ_d^{r},[33,34]

$$\Sigma_{\text{d}}^{\text{r}} = -\text{i}\frac{\Gamma_{\text{d}}}{2}, \tag{7}$$

where Γ_{d} denotes the on-site dephasing strength. Then the corresponding retarded Green's function including the dephasing effect can be written as,

$$G^{\text{r}} = \left[E - H(t) - \Sigma^{\text{r}} - \Sigma_{\text{d}}^{\text{r}} \right]^{-1}. \tag{8}$$

It is reported that the symmetric and asymmetric ZGNRs exhibit completely different transport behaviors under bias although they have similar band structure.[35] In our calculation, both the symmetric ZGNRs with even numbers of zigzag carbon chains and asymmetric ZGNRs with odd numbers of zigzag carbon chains are considered. The width and length of the symmetric (asymmetric) ZGNRs based device are 4.1 nm (3.9 nm) and 14.8 nm, respectively and the energy of the first subband of our proposed ZGNRs ranges from about -0.6 eV to 0.6 eV. In order to study the spatial symmetry of the pumping potential, four different pumping regions with indices $k = 1,2,3,4$ are considered, as shown in Fig. 1(a). The size of each pump region is set to be 1.2 nm $\times$ 5.9 nm and 1.0 nm $\times$ 5.9 nm for the symmetric and asymmetric ZGNRs, respectively.

3. Results and discussion

Figure 2 presents the valley-polarized pumping current $I^{\mathrm{L}}_{kk'}$ as well as the static transmission coefficient of symmetric ZGNRs as a function of the Fermi level E_{f} with a static potential $V_0 = 0.2$ V and a pumping potential $V_{\mathrm{p}} = 50$ mV. Here the subscript kk' denotes different pumping regions. We fix one region of $k = 1$ and change the other region with $k' = 2,3,4$ to study the effect of spatial symmetry on the pumping current. The phase difference of two different pumping regions is set to be $\phi_{kk'} = \pi/2$. It is found that the transmission spectrum of ZGNRs with static pumping potentials shows two major dips which indicate that the transport process is dominated by the quantum resonant effect. As a result, the pumped current shows resonance characteristics near the resonant energy in the static transmission coefficient. For instance, all valley-polarized currents with different pumping regions present a peak at -0.076 eV where a sharp dip of transmission coefficient occurs. Such a resonance-assisted behavior of pumping current is a generic property of electron pump.[36] Moreover, the valley-polarized current I^{L}_{12} with pumping potential $V_{\mathrm{p}}(x,y) = V_{\mathrm{p}}(-x,y)$ shows large values in the whole energy domain and the pumped current changes its sign at about -0.16 eV due to the transmission dip, while the valley-polarized current I^{L}_{14} with the pumping potential $V_{\mathrm{p}}(x,y) = V_{\mathrm{p}}(-x,-y)$ is relatively small and a broad peak is found around -0.16 eV without sign change. The pumped current I^{L}_{13} with the pumping potential $V_{\mathrm{p}}(x,y) = V_{\mathrm{p}}(x,-y)$ is smaller than I^{L}_{14} although their transmission spectrum are almost the same.

In order to study the even–odd effect on pumping current of ZGNRs, the valley-polarized pumping current of asymmetric ZGNRs as a function of the Fermi level with $V_0 = 0.2$ V and $V_{\mathrm{p}} = 50$ mV are calculated and plotted in Fig. 3. The valley-polarized current I^{L}_{12} of asymmetric ZGNRs is similar to that of the symmetric case. For the valley-polarized current I^{L}_{13} of asymmetric ZGNRs with the pumping potential $V_{\mathrm{p}}(x,y) = V_{\mathrm{p}}(x,-y)$ and I^{L}_{14} of asymmetric ZGNRs with the pumping potential $V_{\mathrm{p}}(x,y) = V_{\mathrm{p}}(-x,-y)$, they become much larger than those of symmetric ZGNRs. This is in agreement with the very small saturated current in the symmetric ZGNRs due to the presence of conductance gap around the Fermi level.[35] Especially, it is found that a sign change occurs at $E_{\mathrm{f}} = -0.185$ eV for the valley-polarized pumping current I^{L}_{13}.

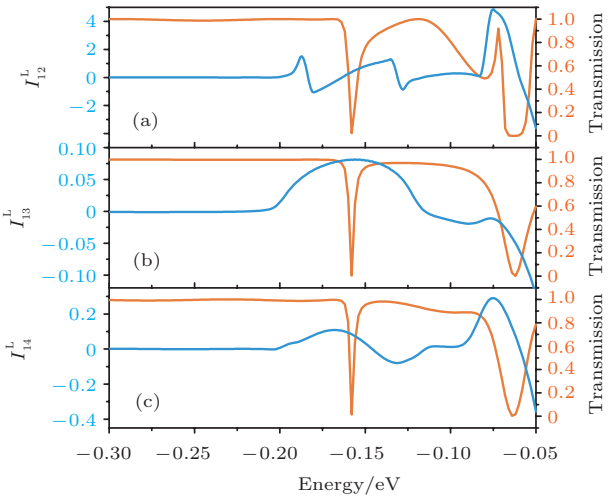


Fig. 2. (color online) Valley-polarized pumping current and transmission coefficient of symmetric ZGNRs as a function of the Fermi level with a static potential $V_0 = 0.2$ V and a pumping potential $V_{\mathrm{p}} = 50$ mV applied on (a) region 1 and region 2, (b) region 1 and region 3, and (c) region 1 and region 4. The initial phase is set to be $\phi_1 = 0$ and $\phi_{k=2,3,4} = \pi/2$.

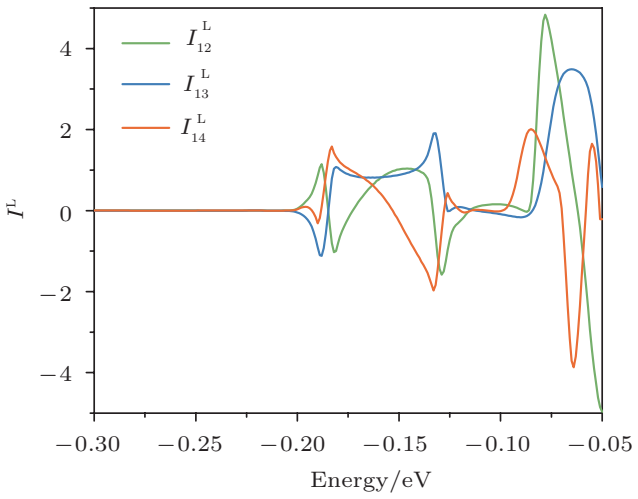


Fig. 3. (color online) Valley-polarized pumping current of asymmetric ZGNRs as a function of the Fermi level with a static potential $V_0 = 0.2$ V and a pumping potential $V_{\mathrm{p}} = 50$ mV applied on different pumping regions. The initial phase is set to be $\phi_1 = 0$ and $\phi_{k=2,3,4} = \pi/2$.

We then examine the relation between the valley-polarized pumping current of symmetric ZGNRs and the phase difference $\phi_{kk'}$ of the pumping potentials at $E_{\mathrm{f}} = -0.076$ eV. As shown in Fig. 4, a sinusoidal behavior is observed for

$I^{\rm L}_{14}$ with the pumping potential $V_{\rm p}(x,y) = V_{\rm p}(-x,-y)$ while it slightly destroyed for $I^{\rm L}_{13}$ with the potential $V_{\rm p}(x,y) = V_{\rm p}(x,-y)$. The sinusoidal behavior cannot hold for $I^{\rm L}_{12}$ which keeps almost zero within the phase difference of $[-\pi,-(3/4)\pi]$ and $[(3/4)\pi,\pi]$. In previous studies, it is reported that the pumping current is proportional to the phase difference, namely, $I^{\rm p}_{kk'} \propto V_{\rm p}\sin\phi_{kk'}$ while this relation dose not hold for large pumping amplitude. In order to demonstrate this relation, we calculate the pumping current $I^{\rm L}_{12}$ with a small pumping amplitude $V_{\rm p} = 10$ meV, as plotted in the inset of Fig. 4. It is found that $I^{\rm L}_{12}$ shows the sinusoidal behavior under a small pumping amplitude. Moreover, a general antisymmetry relation between the pumping current and the phase difference is found for all pumping regions, namely, $I(\phi_{1k}) = -I(-\phi_{1k})$. We also find that the valley-polarized current vanishes when the phase difference is $n\pi$ since two pumping parameters vary simultaneously to enclose a line at $\phi_{1k} = n\pi$. The valley polarization of the pumped current defined as

$$P = \frac{I_K - I_{K'}}{|I_K + I_{K'}|}$$

is then calculated for $I^{\rm L}_{12}$, as shown in Fig. 4. The positive (negative) pumping current in the left lead presents a completely valley polarization with $P = 1$ (-1) since it is fully generated by the valley K (K'). Therefore, the pumping current $I^{\rm L}_{12}$ exhibits a purely valley-polarized current $I_{K'}$ within the phase difference of $[-\pi,0)$ while it is fully contributed by the K valley within the phase difference of $(0,\pi]$.

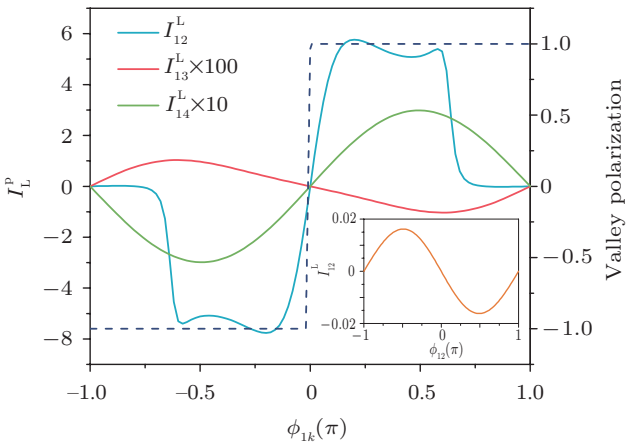


Fig. 4. (color online) Valley-polarized pumping current of symmetric ZGNRs as a function of the phase difference ϕ_{1k} with a static potential $V_0 = 0.2$ V and a pumping potential $V_{\rm p} = 50$ mV at $E_{\rm f} = -0.076$ eV for different spatial symmetries. A factor of 100 and 10 is multiplied to $I^{\rm L}_{13}$ and $I^{\rm L}_{14}$ for illustration, respectively. The dashed blue line denotes the valley polarization of pumping current $I^{\rm L}_{12}$ as a function of the phase difference. Inset: Valley-polarized pumping current $I^{\rm L}_{12}$ as a function of the phase difference ϕ_{12} with a static potential $V_0 = 0.2$ V and a pumping potential $V_{\rm p} = 10$ mV at $E_{\rm f} = -0.076$ eV.

The effect of the pumping amplitude $V_{\rm p}$ on the valley-polarized pumping current is then studied. We calculate the pumping current of symmetric ZGNRs with different pumping potentials and a static potential $V_0 = 0.2$ eV at the resonant energy $E_{\rm f} = -0.076$ eV, as plotted in Fig. 5. The phase difference between two pumping potentials is set to be $\pi/2$. It is found that the valley-polarized current $I^{\rm L}_{12}$ with pumping potential $V_{\rm p}(x,y) = V_{\rm p}(-x,y)$ keeps almost zero when the pumping amplitude is smaller than 0.03 V. It starts to increase rapidly when $V_{\rm p}$ exceeds 0.03 V and reaches the maximum value at $V_{\rm p} = 0.044$ V. Finally, it decreases gradually with the increase of pumping potential. For the pumping current $I^{\rm L}_{13}$, it first decreases slowly with the increasing pumping potential and then decreases linearly when the pumping amplitude exceeds about 0.56 V. The valley-polarized current $I^{\rm L}_{14}$ increases almost linearly with the increase of $V_{\rm p}$. In all cases, we find that the sign of the valley-polarized current does not change by the amplitude of pumping potentials.

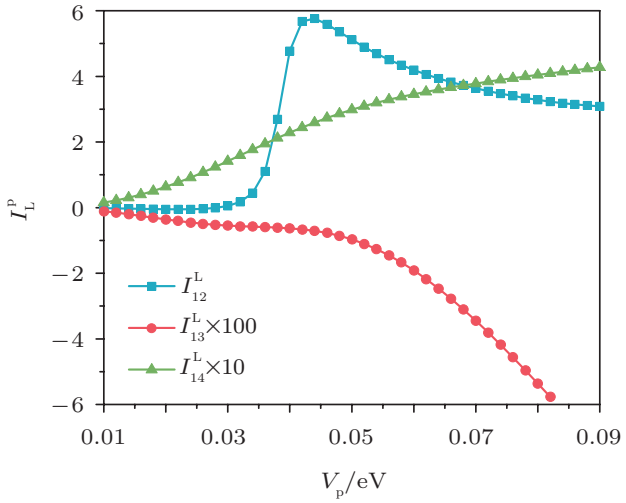


Fig. 5. (color online) Valley-polarized pumping current as a function of the pumping potential $V_{\rm p}$ with a static potential $V_0 = 0.2$ V and a phase difference of $\pi/2$ at $E_{\rm f} = -0.076$ eV for different spatial symmetries. A factor of 100 and 10 is multiplied to $I^{\rm L}_{13}$ and $I^{\rm L}_{14}$ for illustration,respectively.

In order to consider the electron–phonon coupling in the ZGNRs, the dephasing effect is introduced in the parametric pump devices described in Fig. 2. Figure 6 presents the valley-polarized pumping current of symmetric ZGNRs with different dephasing strengths at the Fermi energy of -0.076 eV. We employ the Büttiker dephasing scheme in our present work and the dephasing is modeled by a single parameter $\Gamma_{\rm d}$ which can be considered as the average inelastic broadening parameter to describe the phase-relaxation effects. It is found that the valley-polarized current $I^{\rm L}_{12}$ decreases as the dephasing strength increases and changes the sign at $\Gamma_{\rm d} = 0.1$ eV while $I^{\rm L}_{13}$ increases with the increase of $\Gamma_{\rm d}$. For the pumping current $I^{\rm L}_{14}$ with the pumping potential symmetry $V_{\rm p}(x,y) = V_{\rm p}(-x,-y)$, it first increases and reaches the maximum at $\Gamma_{\rm d} = 0.06$ eV. Then $I^{\rm L}_{14}$ decreases to the minimum at

$\Gamma_d = 0.12$ eV and it finally starts to increase with the increasing dephasing strength.

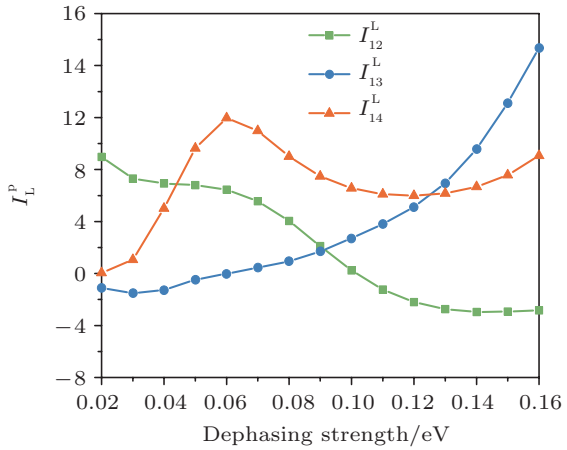


Fig. 6. (color online) Valley-polarized pumping current of symmetric ZGNRs as a function of the dephasing strength Γ_d with a static potential $V_0 = 0.2$ V and a pumping potential $V_p = 50$ mV at $E_f = -0.076$ for different spatial symmetries. The phase difference is set to be $\pi/2$.

4. Conclusion

In conclusion, we have studied the valley-polarized current in symmetric and asymmetric ZGNRs based pump devices. Resonance characteristics are clearly observed for the pumping current near the resonant energy in the static transmission spectrum. Different pumping regions are considered in order to study the effect of spatial symmetry on the valley-polarized current. It is found that the valley-polarized current I_{12}^L generated by pumping potentials $V_p(x,y) = V_p(-x,y)$ is the largest one. Moreover, the valley-polarized currents with the pumping potential symmetry $V_p(x,y) = V_p(x,-y)$ and $V_p(x,y) = V_p(-x,-y)$ of symmetric ZGNRs are much smaller than those of asymmetric ZGNRs. The pumping current I_{13}^L of symmetric ZGNRs decreases with the increase of pumping amplitude V_p while I_{14}^L of symmetric ZGNRs increases with the increasing V_p. The dephasing effect is also studied in symmetric ZGNRs within the Büttiker dephasing scheme and we find that I_{13}^L increases with the increasing dephasing strength Γ_d while I_{14}^L decreases as Γ_d increases. Our theoretical results are helpful to generate and control valley-polarized currents in graphene-based valleytronic devices.

References

[1] Rycerz A, Tworzyd?o J and Beenakker C W J 2007 *Nat. Phys.* **3** 172
[2] Xiao D, Yao W and Niu Q 2007 *Phys. Rev. Lett.* **99** 236809
[3] Peres N M R 2010 *Rev. Mod. Phys.* **82** 2673
[4] Gunlycke D and White C T 2011 *Phys. Rev. Lett.* **106** 136806
[5] Nebel C E 2013 *Nat. Mater.* **12** 690
[6] Gorbachev R V, Song J C W, Yu G L, Kretinin A V, Withers F, Cao Y, Mishchenko A, Grigorieva I V, Novoselov K S, Levitov L S and Geim A K 2014 *Science* **346** 448
[7] Xu X, Yao W, Xiao D and Heinz T F 2014 *Nat. Phys.* **10** 343
[8] Zhang L and Wang J 2014 *Chin. Phys. B* **23** 087202
[9] Tian H Y 2015 *Chin. Phys. B* **24** 127301
[10] Chen X, Zhang L and Guo H 2015 *Phys. Rev. B* **92** 155427
[11] Xu F, Yu Z, Ren Y, Wang B, Wei Y and Qiao Z 2016 *New J. Phys.* **18** 113011
[12] Schaibley J R, Yu H, Clark G, Rivera P, Ross J S, Seyler K L, Yao W and Xu X 2016 *Nat. Rev. Mater.* **1** 16055
[13] Yu Z, Xu F and Wang J 2016 *Carbon* **99** 451
[14] Zhang L, Yu Z, Xu F and Wang J 2018 *Carbon* **126** 183
[15] Shimazaki Y, Yamamoto M, Borzenets I V, Watanabe K, Taniguchi T and Tarucha S 2015 *Nat. Phys.* **11** 1032
[16] Zhang L, Gong K, Chen J, Liu L, Zhu Y, Xiao D and Guo H 2014 *Phys. Rev. B* **90** 195428
[17] Yu Y, Zhou Y, Wan L, Wang B, Xu F, Wei Y and Wang J 2016 *Nanotechnology* **27** 185202
[18] Brouwer P W 1998 *Phys. Rev. B* **58** R10135
[19] Makhlin Y and Mirlin A D 2001 *Phys. Rev. Lett.* **87** 276803
[20] Wang B, Wang J and Guo H 2003 *Phys. Rev. B* **68** 155326
[21] Li C, Yu Y, Wei Y and Wang J 2007 *Phys. Rev. B* **75** 035312
[22] Xu F, Xing Y and Wang J 2011 *Phys. Rev. B* **84** 245323
[23] Xing Y, Wang B, Wei Y, Wang B and Wang J 2004 *Phys. Rev. B* **70** 245324
[24] Zhang Q, Chan K S and Lin Z 2011 *Appl. Phys. Lett.* **98** 032106
[25] Chen M N, Sheng L, Shen R, Sheng D N and Xing D Y 2015 *Phys. Rev. B* **91** 125117
[26] Deng W Y, Luo W, Geng H, Chen M N, Sheng L and Xing D Y 2015 *New J. Phys.* **17** 103018
[27] Marcellino J T J, Wang M J, Wang S K and Wang J 2018 *Chin. Phys. B* **27** 057801
[28] Wang J and Liu J F 2017 *Phys. Rev. B* **95** 205433
[29] Jiang Y, Low T, Chang K, Katsnelson M I and Guinea F 2013 *Phys. Rev. Lett.* **110** 046601
[30] Wang J, Chan K S and Lin Z 2014 *Appl. Phys. Lett.* **104** 013105
[31] Castro Neto A H, Guinea F, Peres N M R, Novoselov K S and Geim A K 2009 *Rev. Mod. Phys.* **81** 109
[32] Büttiker M 1993 *J. Phys.: Condens. Matter* **5** 9361
[33] Büttiker M 1986 *Phys. Rev. B* **33** 3020
[34] Xing Y, Sun Q F and Wang J 2008 *Phys. Rev. B* **77** 115346
[35] Li Z, Qian H, Wu J, Gu B L and Duan W 2008 *Phys. Rev. Lett.* **100** 206802
[36] Wei Y, Wang J and Guo H 2000 *Phys. Rev. B* **62** 9947